Sites NGHP-01-11

By T. Collett, M. Riedel, J. Cochran, R. Boswell, J. Presley, P. Kumar, A. Sathe,
A. Sethi, M. Lall, and the National Gas Hydrate Program Expedition 01 Scientists

Scientific Investigations Report 2012–5054

U.S. Department of the Interior
U.S. Geological Survey

Contents

Figures

Site NGHP-01-11

By T. Collett, M. Riedel, J. Cochran, R. Boswell, J. Presley, P. Kumar, A. Sathe, A. Sethi, M. Lall, and the National Gas Hydrate Program Expedition 01 Scientists

Background and Objectives

Site NGHP-01-11 (Prospectus Site GDGH12-A) is located at 15° 59.4601' N, 81° 59.5290' E in the Krishna-Godavari (KG) Basin (fig. 1). The water depth is ~1,007m. This site was not selected as a primary coring site after LWD/MWD data acquisition was completed.

The objectives of the work carried out at this site follow the general objectives of NGHP Expedition 01, with a focus on the LWD/MWD operations only:

4. Study the occurrence of gas hydrate and establish the background geophysical baselines for gas-hydrate studies;
5. Define the relationship between the sedimentology and structure of the sediments and the occurrence and concentration of gas hydrate;
6. Calibrate remote sensing data such as seismic data by acquiring LWD/MWD data.

Site NGHP-01-11 is located along seismic line AD-94-27 (shot point 298, figs. 2 and 3). This line shows a widespread BSR that is especially well defined where it cross-cuts sedimentary strata (shotpoints 210–330). The depth of the BSR at Site NGHP-01-11 is estimated at ~150 mbsf based on a seismic velocity of 1,580 m/s and a 0.19 s TWT. The BSR depth becomes shallower towards the NW as water depth decreases.

Originally, the site location was chosen at shot point 318 of seismic line AD-94-27, but was subsequently moved to location GDGH12-A to drill through steeply dipping sedimentary strata within the GHSZ field, seen between shot points 275 and 310. Location GDGH12-A also avoids bright sub-BSR reflectivity indicating the possible presence of free gas. Maximum hole penetration at Site NGHP-01-11 was set to 200 mbsf.

About 2 km upslope of Site NGHP-01-11, a series of three seafloor slumps are identified that can potentially form a hazard. The slump-features are characterized by the absence of internal reflectivity between seafloor and BSR, whereas immediately below the BSR a series of bright, dipping reflections can be identified.

Operations

This operations summary covers the transit from Site NGHP-01-10 (GD-3-1) to Site NGHP-01-11 (GDGH12-A) and LWD/MWD drilling operations in Hole NGHP-01-11A (fig. 4). Schedule details and statistics for this site can be found as Appendixes:

- Appendix 1: NGHP Expedition 01 Operations Schedules
- Appendix 2: NGHP Expedition 01 Operations Statistics

Included in the "Methods" chapter and the glossary is a list of standard or commonly used operations terms and acronyms

Hole NGHP-01-11A

The 11.9 NMI transit from Site NGHP-01-10 to Site NGHP-01-11 was completed in 1.4 hours at an average speed of 8.0 knots.

The first and only hole of Site NGHP-01-11 was drilled on Leg 2 of NGHP Expedition 01 as the 11th hole of a 12-hole LWD/MWD transect. The sea voyage ended at 2300 hr on June 3, 2006, and once thrusters were down, the vessel was switched over to DP control. A positioning beacon was deployed at the Hole NGHP-01-11A location coordinates at 0001 hr on June 4, 2006. The LWD/MWD tools, consisting of the GeoVISION (RAB), EcoScope, SonicVISION, and TeleScope, were assembled. The replacement ProVISION NMR tool, put aboard during the supply boat rendezvous en route to Site NGHP-01-10, was also included in the tool string. The LWD/MWD tools were lowered to 80.0 mbrf where a flow test was conducted. The Minitron was then turned on and the drill string was lowered to the seafloor. A tag of the seafloor indicated a mudline depth of 1,018.0 mbrf. For reference, the PDR depth at this site, adjusted to the rig floor DES, was 1,032.4 mbrf. After offsetting the vessel 2 meters N of the site coordinates, Hole NGHP-01-11A was spudded at 0352 hr on June 4, 2006. LWD/MWD operations continued at an "average" controlled rate of 34.8 m/h (or 25.8 m/h average net ROP including connection time). This hole was actually drilled at two different target rates varying between 50 m/h and 30 m/h to a total depth of 200.0 mbsf. The slower ROP was used to better characterize gas hydrate "zones of interest". The hole was displaced with 56 barrels of 10.5 ppg mud, the top drive was set back, and the drill string was pulled clear of the seafloor at 1256 hr on June 4th. The drill pipe was partially recovered and hung-off on knobby joints positioning the EOP at a depth of 791.8 mbrf. All hydrophones were raised and the positioning beacon was recovered. At 1345 hr on June 4th, the vessel began moving in DP mode with the drill pipe suspended to Site NGHP-01-05 (KGGH02-A). This completed operations at Site NGHP-01-11.

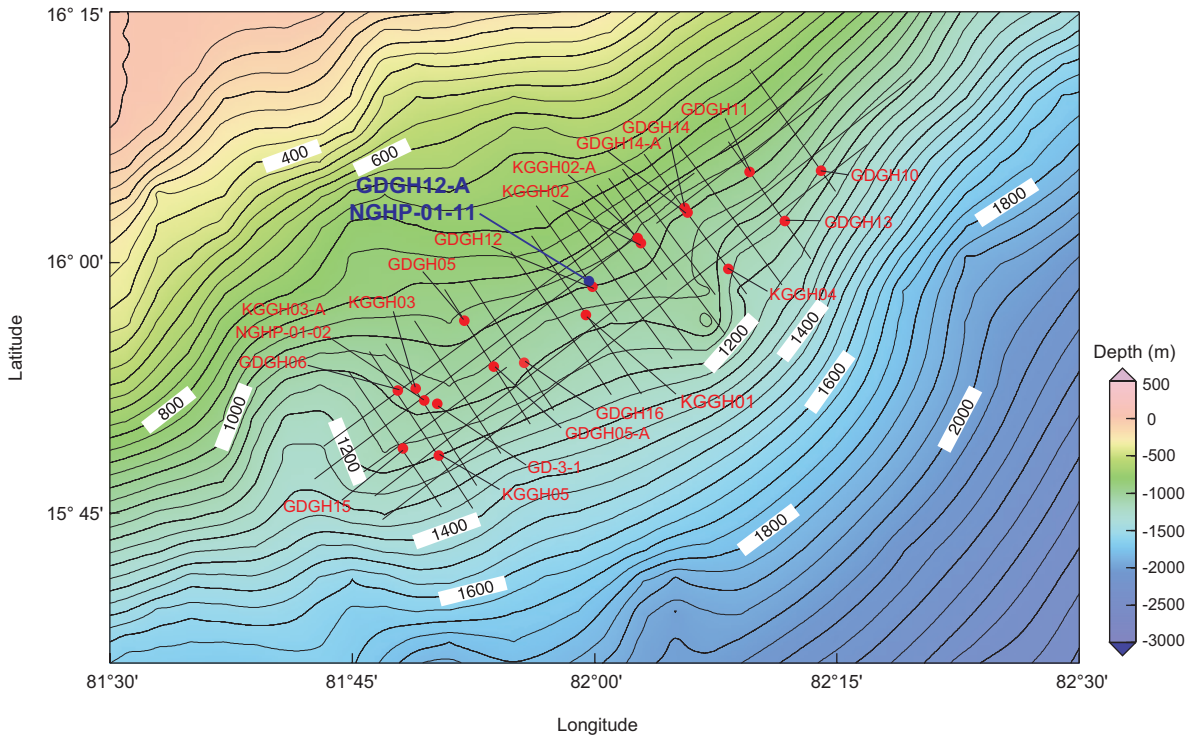

Figure 1. Location of Site NGHP-01-11 (Prospectus Site GDGH12-A) in the Krishna-Godavari (KG) Basin.

Downhole Logging

Logging While Drilling

Operations

After tagging the seafloor at 1,018 mbrf (driller's depth), Hole NGHP-01-11A was spudded at 0352 hr on June 4, 2006. LWD tools in the BHA included the GeoVISION resistivity, the EcoScope, the SonicVISION, the TeleScope MWD, and the ProVISION NMR tools. For details on each LWD tool and the measurements it makes, see the "Downhole Logging" section in the "Methods" chapter.

To avoid washing out the formation near the seafloor, Hole NGHP-01-11A was spudded at a relatively low flow rate. The first 10 m were drilled at 100 gpm with a rotation rate of 20 rotations per minute (rpm) and a target rate of penetration (ROP) of 50 m/h. Below 10 mbsf, the rotation rate was increased to 30 rpm; at 30 mbsf, it was increased to 60 rpm and the flow rate was increased until the LWD tools turned on (~370 gpm). Because of time constraints, we started drilling at a relatively high ROP of 50 m/h. We then slowed down at about 80 mbsf to a target ROP of 30 m/h to maximize data quality. The target depth of 201 mbsf (1,219 mbrf) was reached at 1140 hr on June 4th. After completing Hole NGHP-01-11A, we cleared the seafloor at 1256 hr, pulled the bit to 800 mbrf, and moved in dynamic positioning by about 4 nautical miles to the location of Hole NGHP-01-05B. Depths in mbsf are referenced to the seafloor depth tagged by the driller.

Gas Monitoring with Real Time LWD/MWD Data

The LWD logs were acquired in the first hole drilled at Site NGHP-01-11 to plan coring and pressure coring operations in subsequent holes. As Hole NGHP-01-11A was drilled without coring, the LWD data had to be monitored for safety to detect gas entering the wellbore. As explained in the "Downhole Logging" section of the "Methods" chapter, the primary measurement used for gas monitoring was the "annular pressure while drilling" (APWD) measured by the EcoScope tool in the borehole annulus. We looked for sudden decreases of more than 100 psi in the annular pressure, which could be due to low-density gas entering the wellbore. We also monitored pressure increases of the same magnitude, which could be due to fluid acceleration caused by a gas kick (Aldred and others, 1998).

Figure 5 shows the measured borehole fluid pressure profile in Hole NGHP-01-11A after subtraction of the hydrostatic pressure trend. This residual pressure shows only minor fluctuations that are well below the 100 psi level that would have required preventive action. We also monitored the coherence of the sonic waveforms acquired by the SonicVISION tool,

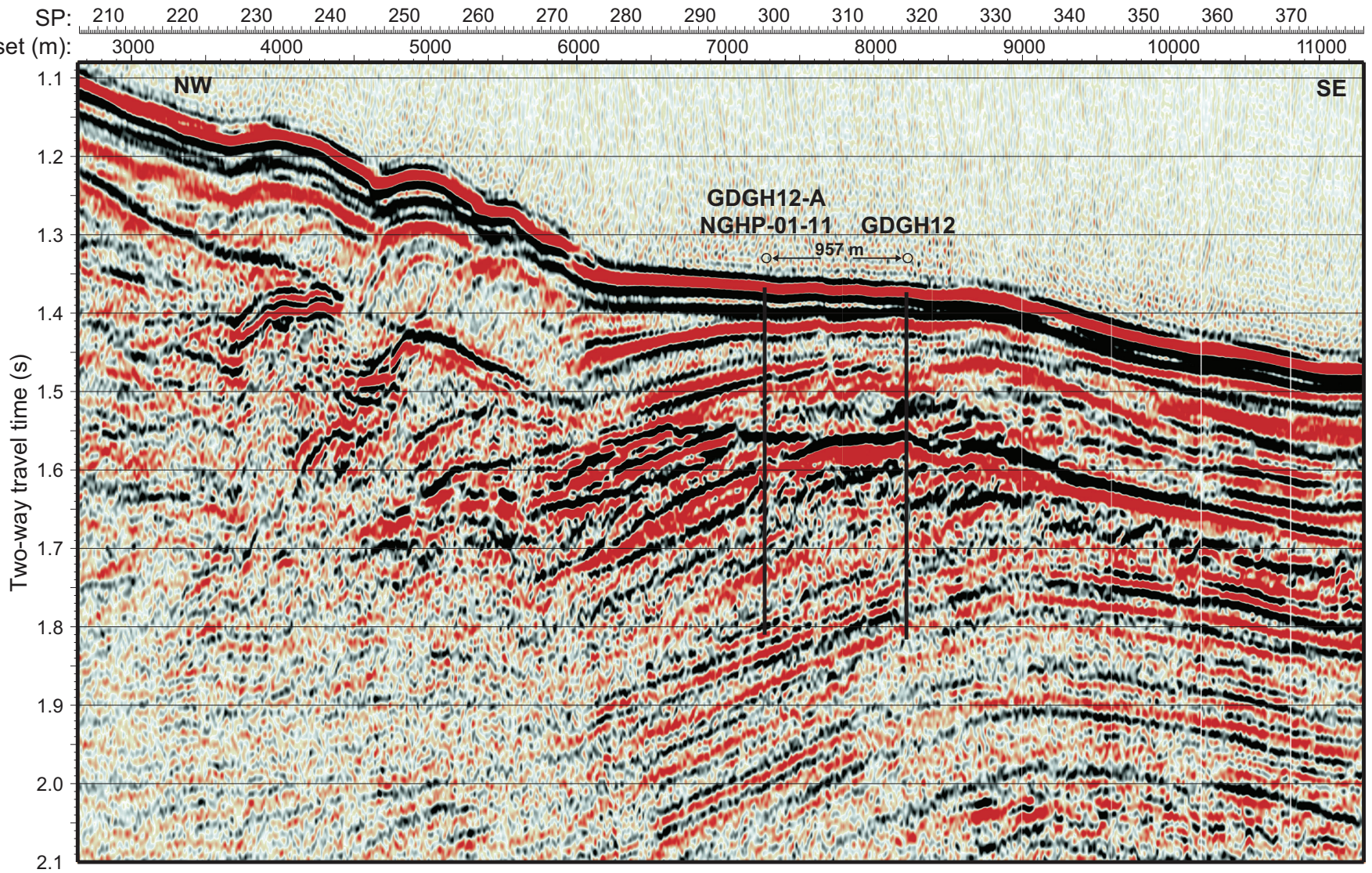

Figure 2. Section of 2D seismic line AD-94-27 around Site NGHP-01-11 (Prospectus Site GDGH12-A) showing a broad basin and an extensive BSR occurrence. Site NGHP-01-14 is also located along this line, about 8 km upslope to the NW. [BSR, bottom-simulating reflector]

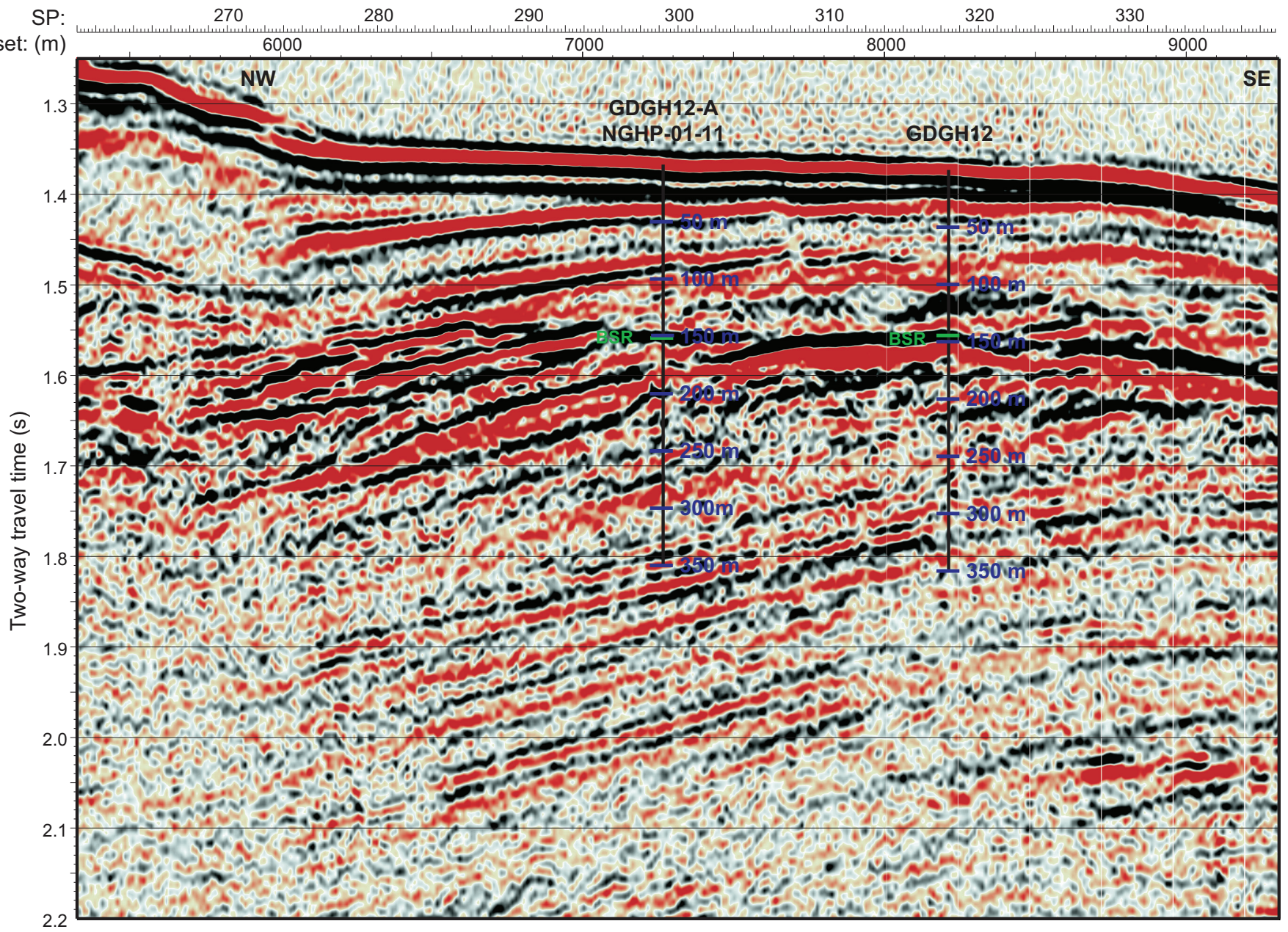

Figure 3. Section of seismic line AD-94-27 around Site NGHP-01-11 (Prospectus Site GDGH12-A) showing predicted formation tops and BSR depth (~150 mbsf) based on a uniform seismic velocity of 1,580 m/s. [BSR, bottom-simulating reflector]

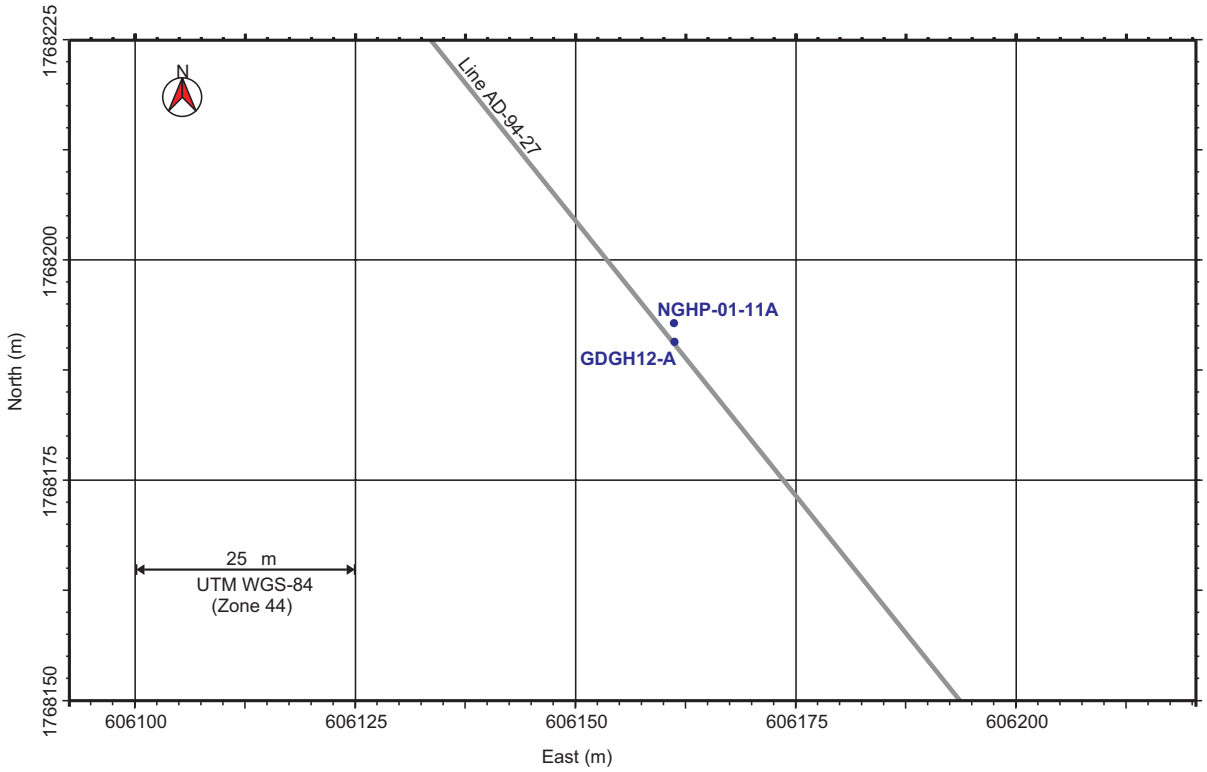

Figure 4. Map showing the hole occupied at Site NGHP-01-11 (GDGH12-A).

configured to capture the borehole fluid wave. Gas indicators are loss of coherence in the waveforms and a slower sound velocity for the drilling fluid. We found no significant decrease of sonic waveform coherence or fluid velocity throughout the interval drilled.

LWD Log Quality

Figure 5 also shows the quality control logs for Hole NGHP-01-11A. The two curves for rate of penetration are an instantaneous rate of penetration (ROP_RM) and a rate of penetration averaged over the last five feet (ROP5_RM). The occasional peaks in the instantaneous rate of penetration are artifacts due to depth fluctuations during pipe connections. Because of time constraints, we started drilling Hole NGHP-01-11A with a ROP around 50 m/h and decreased it to around 30 m/h below 80 mbsf, which is sufficient to record high resolution GeoVISION resistivity images and ProVISION NMR data (for details, see "Downhole Logging" in the "Methods" chapter).

The density (DCAV) and ultrasonic caliper logs (UCAV) show an enlarged hole near the seafloor (20–50 mbsf), with a hole diameter up to 12 in. The bit size (dashed line in fig. 5) is 9 7/8 in, and the ultrasonic caliper shows that most of the borehole below 50 mbsf is just above 10 in. The density caliper, however, shows a borehole that is smaller than the bit size for most of the interval 100–140 mbsf; the ultrasonic caliper is a direct measurement of borehole size and is probably more reliable. The density correction, calculated from the difference between the short- and long-spaced density measurements, is everywhere within the interval 0–0.2 g/cm^3 (fig. 5), suggesting that the density measurements should be of good quality.

Figure 6 is a summary of the LWD gamma ray, density, neutron porosity, and resistivity logs measured in Hole NGHP-01-11A. (SonicVISION and ProVISION results are not shown) The gamma ray and resistivity logs measured by the GeoVISION and EcoScope generally agree. The GeoVISION and EcoScope gamma ray curves have the same shape, but are offset by about 20–30 gAPI; this difference is most likely due to tool calibration.

Figure 7 shows a comparison of the ring resistivity measured by the GeoVISION with the attenuation and phase resistivity curves obtained by the EcoScope tool at different frequencies and transmitter-receiver spacings. For a given transmitter-receiver spacing, the phase-shift EcoScope resistivities have higher vertical resolution than the attenuation resistivities and thus show more detail.

Figure 6 also shows two bulk density curves: RHOB is the average density obtained by the EcoScope tool while rotating, while IDRO (image-derived density) is the value of density measured when the sensors were in closest contact with the formation. The two density curves are generally close, except for a few intervals (for example, 40–46 mbsf) where the image-derived density is greater.

The bottom-simulating reflector (BSR) that should mark the bottom of the gas hydrate stability zone was estimated to be at a depth of 150 mbsf in this hole. Above this depth,

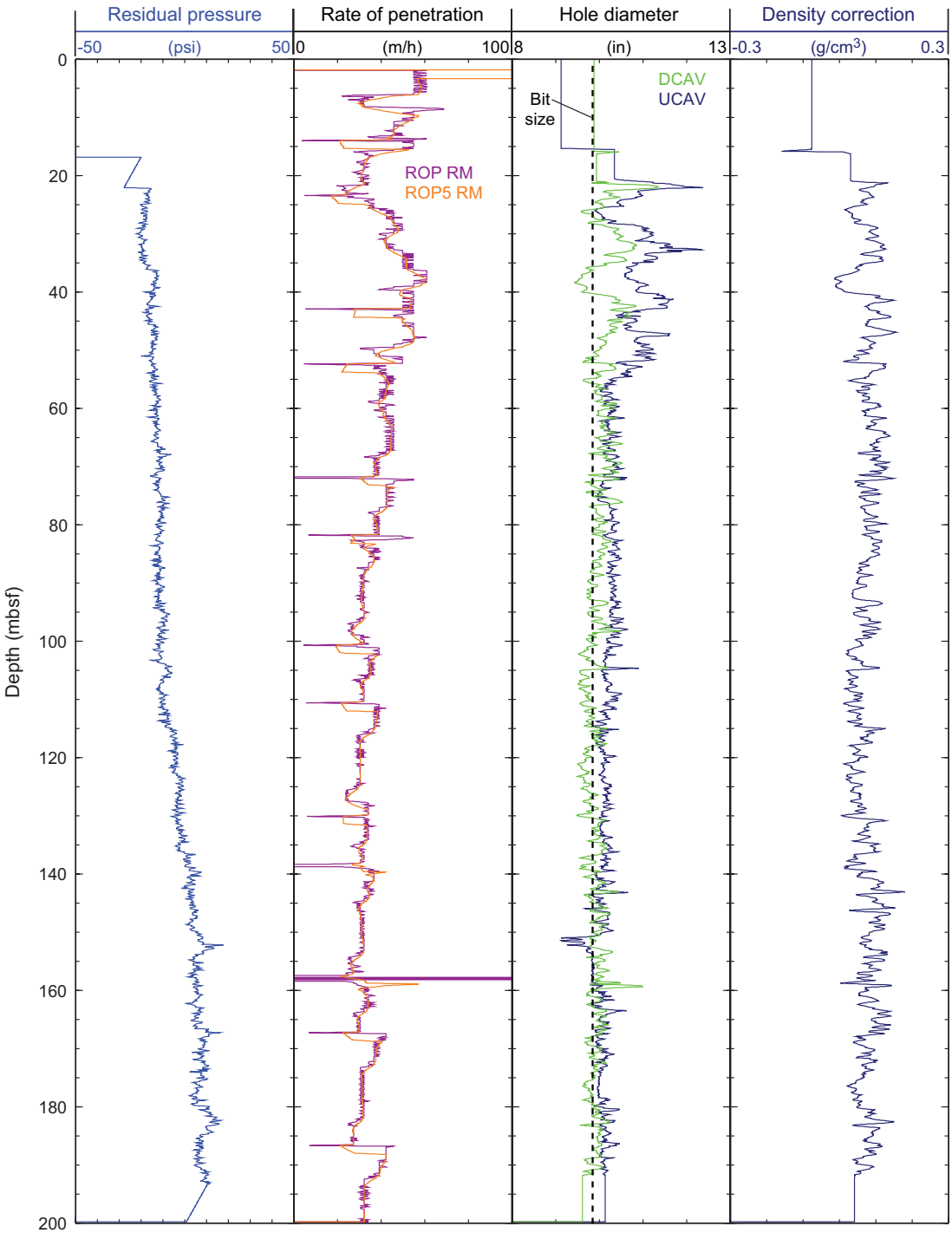

Figure 5. Monitoring and quality-control LWD/MWD logs from Hole NGHP-01-11A. [LWD/MWD, logging-while-drilling/measuring-while-drilling; ROP_RM, Instantaneous rate of penetration; ROP5_RM, Rate of penetration averaged over a 5-ft interval; UCAV, Ultrasonic caliper; DCAV, density caliper]

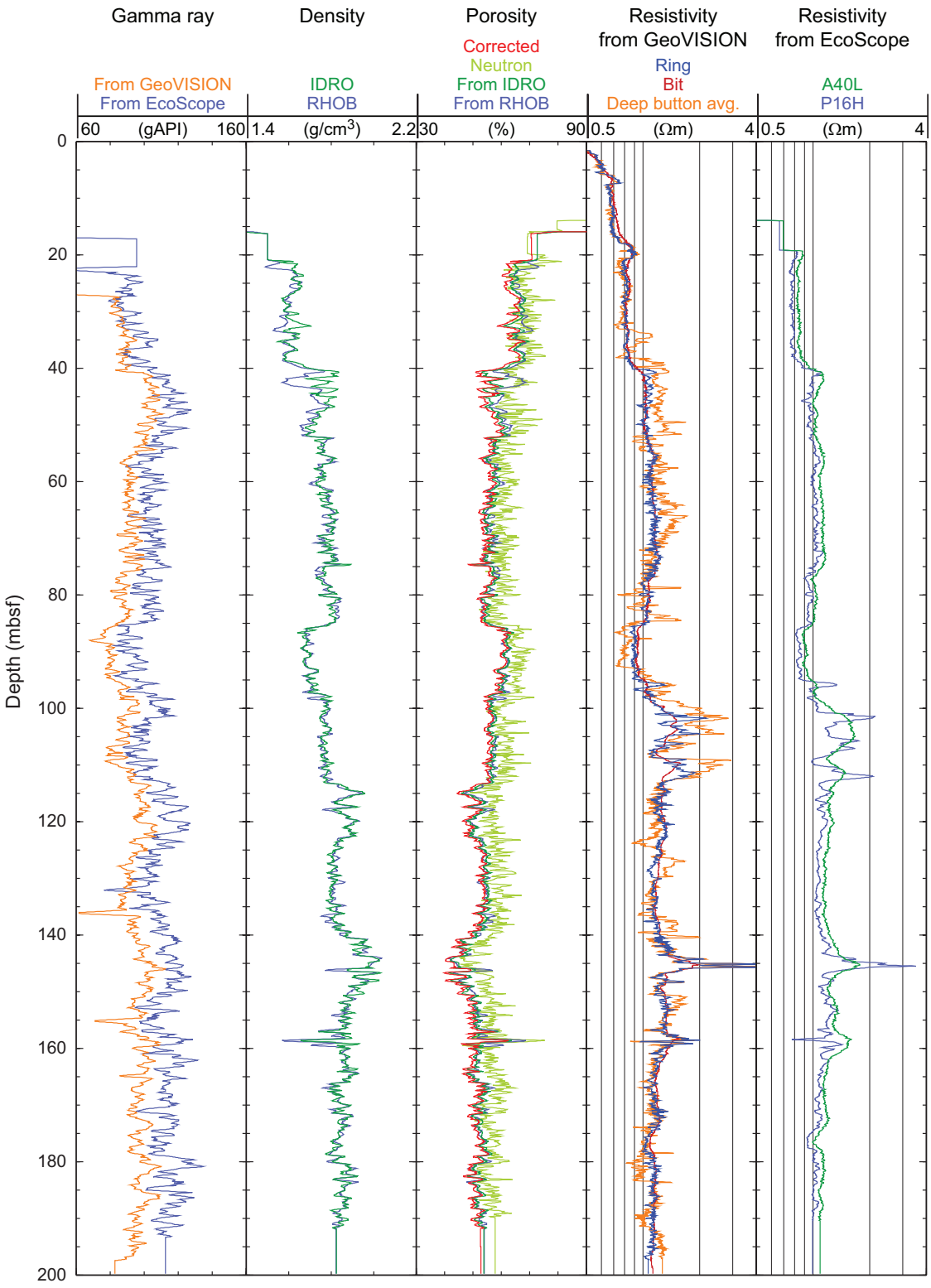

Figure 6. Summary of LWD log data from Hole NGHP-01-11A. [LWD, logging while drilling; gAPI, American Petroleum Institute gamma ray units; IDRO, Image-derived density (EcoScope); RHOB, Bulk density (EcoScope); neutron, Thermal neutron porosity (EcoScope); corrected density, density porosity with core derived grain densities (EcoScope); RING, Ring resistivity (GeoVISION); BIT, Bit resistivity (GeoVISION); Deep Button avg., Button deep resistivity (GeoVISION); A40L, Attenuation resistivity measured at 400 kHz and a transmitter-receiver spacing of 40 in (EcoScope); and P16H, Phase-shift resistivity at 2 MHZ and a transmitter-receiver spacing of 16 in (EcoScope)]

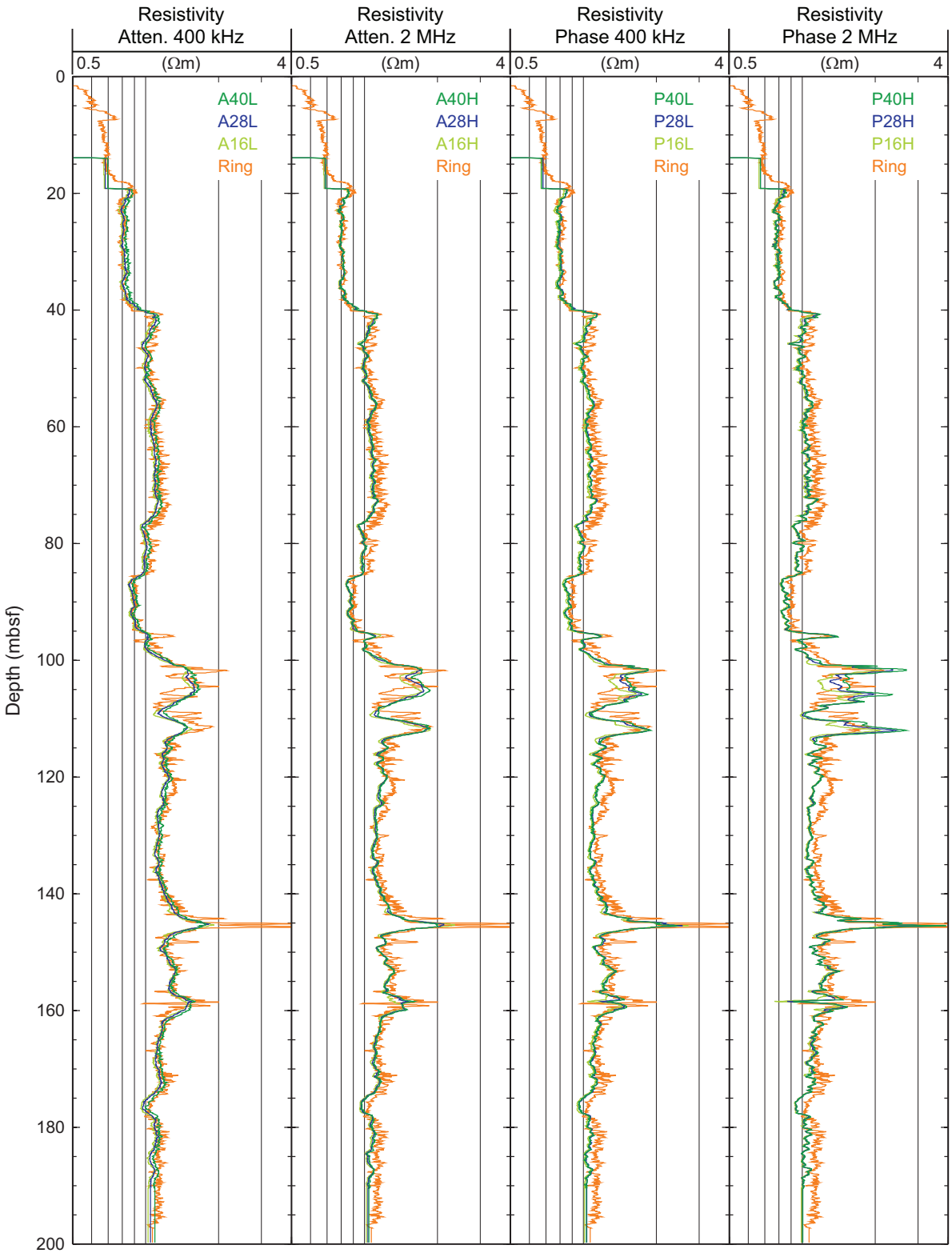

Figure 7. Comparison of LWD resistivity curves from Hole NGHP-01-11A. [LWD, logging while drilling; Ring, Ring resistivity (GeoVISION); AXXL, Attenuation resistivity measured at a frequency of 400 kHz, where XX is the transmitter-receiver spacing in inches (EcoScope); AXXH, Attenuation resistivity measured at a frequency of 2 MHz, where XX is the transmitter-receiver spacing in inches (EcoScope); PXXL, Phase-shift resistivity measured at a frequency of 400 kHz, where XX is the transmitter-receiver spacing in inches (EcoScope); PXXH, Phase-shift resistivity measured at a frequency of 2 MHz, where XX is the transmitter-receiver spacing in inches (EcoScope)]

at 145 mbsf, there is a resistivity peak probably due to gas hydrate (see below), but there is no clear change in the LWD logs at or below the BSR depth.

The depths relative to seafloor were fixed for all of the LWD logs by identifying the step change in the GeoVISION gamma ray log at the seafloor. For Hole NGHP-01-11A, the gamma ray logging pick for the seafloor was at a depth of 1,019 mbrf, 1 m deeper than the initial depth estimated by the drillers (1,018 mbrf). The rig floor logging datum was located 10.5 m above sea level.

LWD Porosities

Sediment porosities were calculated from the LWD density and neutron logs in Hole NGHP-01-11A. No core-derived physical property data were available at this site to calibrate and evaluate the log-derived porosities.

The LWD log-derived density measurements from Hole NGHP-01-11A were used to calculate sediment porosities (ϕ) with the standard density-porosity relation: $\phi = (r_g - r_b) / (r_g - r_w)$. We first used a constant water density (r_w) of 1.03 g/cm^3 and a grain/matrix density (r_g) equal to 2.75 g/cm^3. The density log-derived porosities from Hole NGHP-01-11A range from about 65 percent at 20 mbsf to just above 40 percent around 144 mbsf (fig. 6). The density porosities in figure 6 have been calculated from both the bulk density (RHOB) and from the image-derived density curve (IDRO).

In order to estimate the influence of variable grain density, but without any core sample measurements available at this site, we calculated a "corrected porosity" from the IDRO density log and using a least square fourth order polynomial fit with depth of the grain density measurements made on samples from nearby Sites NGHP-01-03 and NGHP-01-05. The results in figure 6 show only minor differences from the original density porosity derived with constant grain density.

The LWD neutron porosity log from Hole NGHP-01-11A (fig. 6) yielded sediment porosities ranging from an average value of about 70 percent at 20 mbsf to about 50 percent around 144 mbsf. Porosities measured by the neutron log are expected to be higher than those computed from the density log in clay-rich sediments, because the neutron log essentially quantifies hydrogen abundance, and counts hydrogen in clay minerals as porosity. The neutron porosity measured by the EcoScope tool shown in figure F6 is the "best thermal neutron porosity" (BPHI); it has been corrected so that the effect of clay is reduced (Adolph and others, 2005), and it is only marginally higher than the density porosity.

LWD Borehole Images

The GeoVISION and EcoScope LWD tools generate high-resolution images of borehole log data. The EcoScope tool produces images of density and hole radius (computed on the basis of the density correction, which depends on the borehole standoff). The GeoVISION produces a gamma ray image and resistivity images with shallow, medium and deep depth of investigation.

Figure 8 shows some of the LWD images collected by the EcoScope and GeoVISION tools. It should be noted that the display in figure 7 is highly compressed in the vertical direction. The unwrapped images are about 80 cm wide (for a 10 in diameter borehole) and the vertical scale is compressed relative to the horizontal by a factor of about 55:1. These high-resolution images can be used for detailed sedimentological and structural interpretations and to image gas-hydrate distribution in sediments (for example, in layers, nodules, fractures). Gas-hydrate-bearing sediments exhibit high resistivities within intervals of uniform or low bulk density. Layers with high resistivities and high densities are likely to be low porosity, compacted, or carbonate-rich sediments. The two resistivity images in figure 8 correspond to two depths of investigation (see "Downhole Logging" in the "Methods" chapter).

The main features of interest in the borehole images are the "bright" high-resistivity layers in the intervals 98–112 mbsf and 144–146 mbsf. These high resistivities do not correspond to high densities in the density image and thus are likely to be local gas-hydrate accumulations.

Gas-Hydrate and Free Gas Occurrence

As previously discussed (see "Downhole Logging" in the "Methods" chapter), the presence of gas hydrate is generally characterized by increases in electrical resistivity and acoustic velocity that are not accompanied by a corresponding porosity decrease. A decrease in porosity alone in water-saturated sediment can result in an increase in resistivity and acoustic velocity. Resistivities logged in Hole NGHP-01-11A show a general negative correlation with porosity (fig. 6), except in the intervals 95–113 mbsf and 144–146 mbsf, where high resistivities suggest that gas hydrate is present.

To make a quantitative estimate of the amount of gas hydrate at Site NGHP-01-11, we followed the procedure described in "Downhole Logging" in the "Methods" chapter, to apply the Archie relationship to the resistivity and porosity logs recorded in Hole NGHP-01-11A.

The procedure and the results are shown in figure 9. The pore fluid resistivity (R_w) was estimated from Fofonoff (1985) using a linear temperature profile derived from the *in situ* temperature measurements at nearby Sites NGHP-01-03 and NGHP-01-05 (6.7 °C at the seafloor; gradient of 42 °C/km) and a water salinity defined by a least square polynomial fit with depth of the values measured on pore water samples from Sites NGHP-01-03 and NGHP-01-05. The estimated m curve is derived from R_w, the porosity (ϕ) and resistivity (R_t) logs ($m_{est} = -\log F / \log\phi$, where $F = R_t / R_w$). As this relationship is defined for water-saturated sediments, the chosen value of $m = 2.1$ is given by the baseline of this curve in the low-resistivity intervals where there is likely no gas hydrate. Using

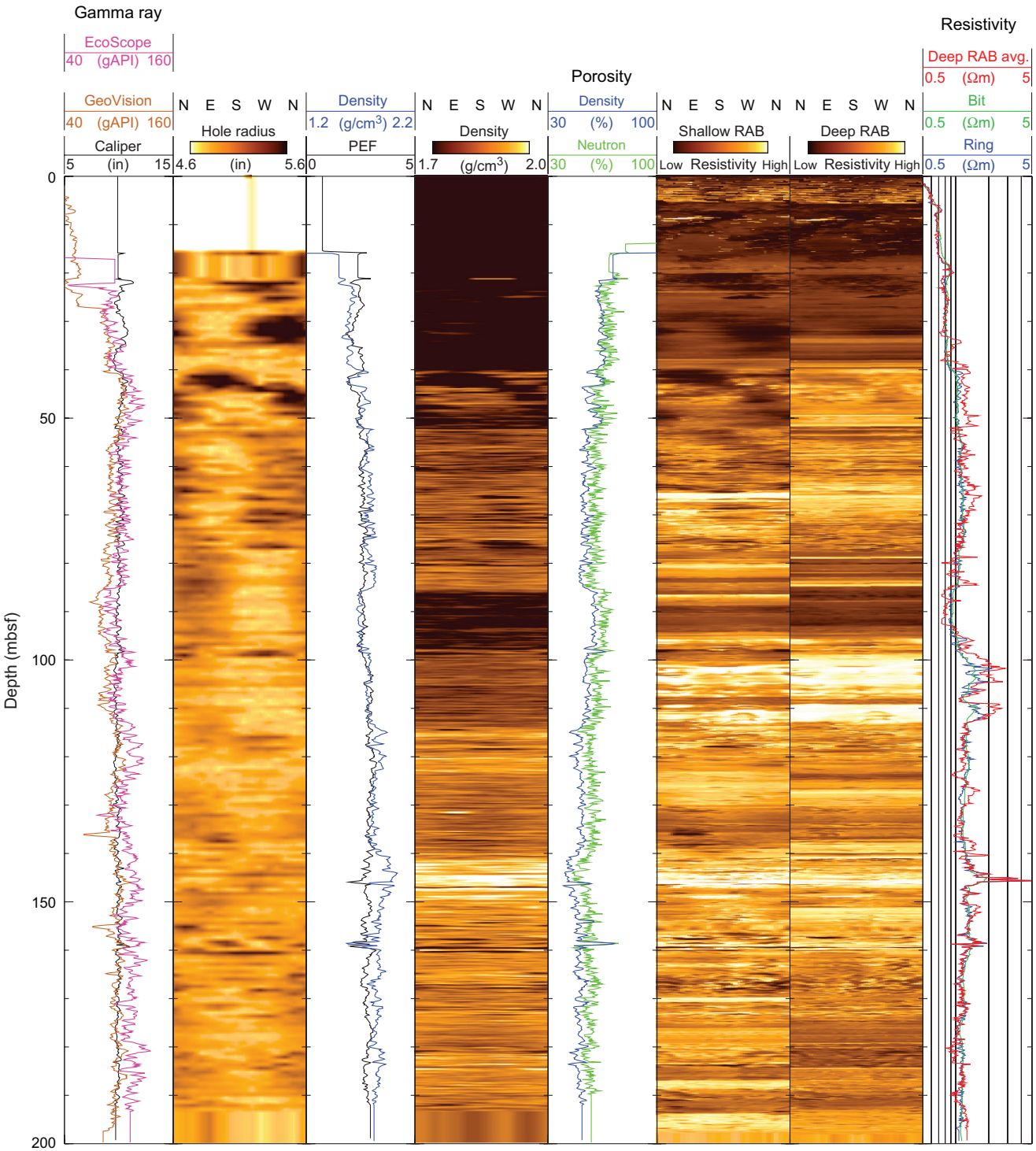

Figure 8. LWD image data from Hole NGHP-01-11A. [LWD, logging while drilling; gAPI, American Petroleum Institute gamma ray units; RAB, Resistivity-At-Bit image obtained by the GeoVISION tool]

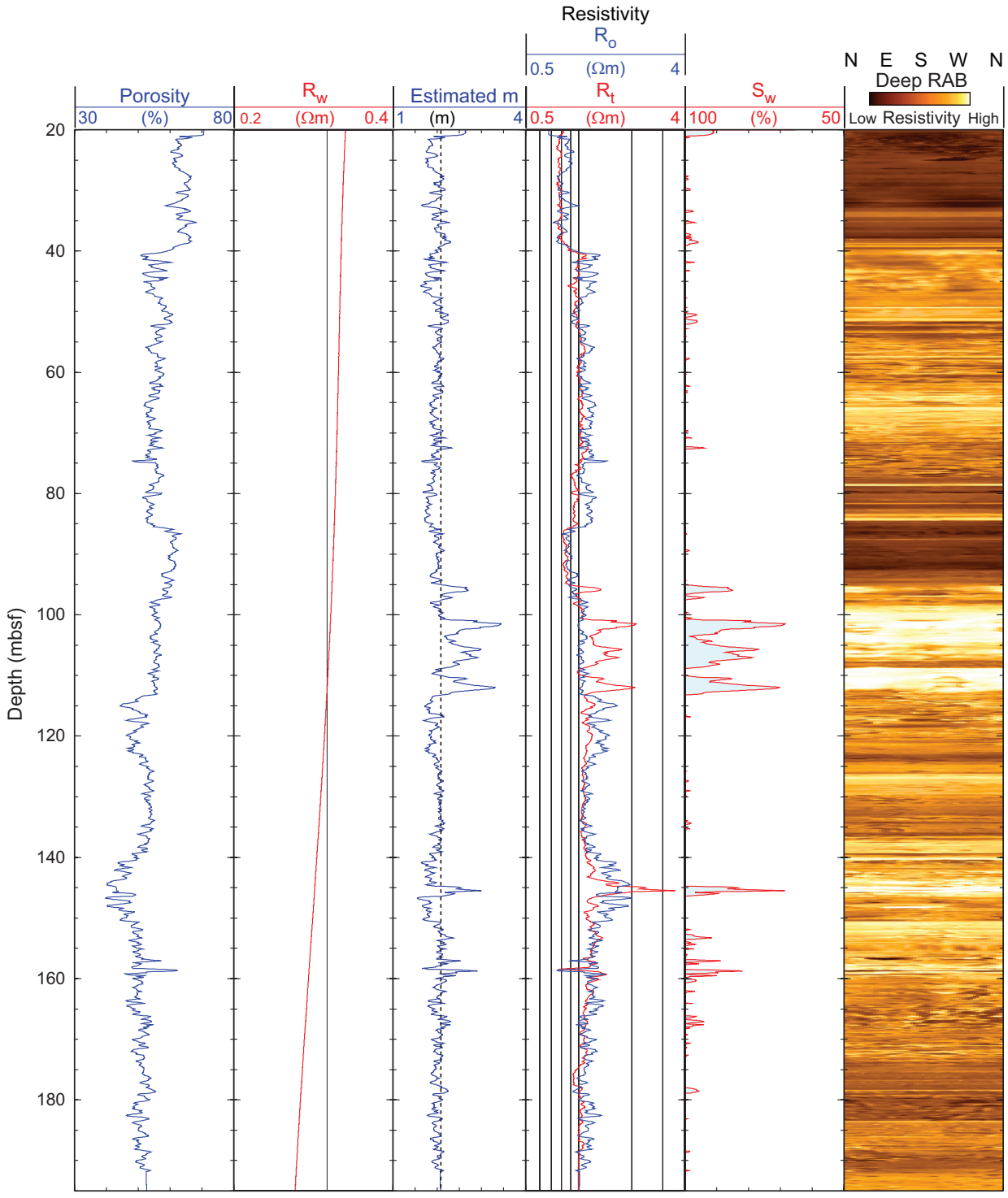

Figure 9. Water saturations from Archie's equation and LWD porosity and resistivity logs in Hole NGHP-01-11A. [LWD, logging while drilling; R_w, Formation water resistivity; R_0, Computed formation resistivity for 100 percent water saturation; R_t, Measured resistivity; S_w, water saturation]

the porosity log and Archie's equation ($R_0 = (a\ R_w)\ /f^m$), we derive the predicted resistivity of the water-saturated formation R_O. A qualitative influence of gas hydrate on the resistivity log is indicated by the difference between the R_0 and the measured resistivity R_t. The estimated water saturation, assumed to be the numerical complement of the hydrate saturation, is $S_w = (R_0/R_t)^{1/n}$, where n=2 (Pearson and others, 1983). We used the "corrected" density porosity computed from the image-derived density (IDRO) and the resistivity from the 16 in, phase-shift, high-frequency propagation resistivity (P16H) measured by the EcoScope tool. We use the P16H curve because it is the resistivity with the highest vertical resolution measured by the EcoScope.

The strongest evidence for gas hydrate is in the interval 95–113 mbsf, where the computed gas-hydrate saturation reaches a maximum of about 35 percent (fig. 9). This interval is also where borehole images show prominent high-resistivity layers (fig. 7). There is also a thin high-resistivity interval at 144–146 mbsf that does not coincide with a density high and that shows a maximum computed gas-hydrate saturation of 35 percent. Outside of these intervals, there is no strong evidence for gas hydrate.

References Cited

Adolph, B., Archer, M., Codazzi, D., el-Halawani, T., Perciot, P., Weller, G., Evans, M., Grant, J., Griffiths, R., Hartman, D., Sirkin, G., Ichikawa, M., Scott, G., Tribe, I., and White, D., 2005, No more waiting—Formation evaluation while drilling: Oilfield Review, Autumn 2005, p. 4–21.

Aldred, W., Cook, J., Bern, P., Carpenter, B., Hutchinson, M., Lovell, J., Rezmer-Cooper, I., and Leder, P.C., 1998, Using downhole annular pressure measurements to improve drilling performance: Oilfield Review, Winter 1998, p. 40–55.

Fofonoff, N.P., 1985, Physical properties of seawater: Journal of Geophysical Research, v. 90, no. C2, p. 3332–3342.

Pearson, C.F., Halleck, P.M., McGuire, P.L., Hermes, R., and Mathews, M., 1983, Natural gas hydrate deposits—A review of *in situ* properties: Journal of Physical Chemistry, v. 87, p. 4180–4185.